for ***Polymer Degradation and Stability***

Effects of MgO Catalyst on Depolymerization of Poly-L-lactic Acid to L,L-Lactide

Toru Motoyama,[a,b] *Takayuki Tsukegi,*[a,b] *Yoshihito Shirai,*[b] *Haruo Nishida,**[a] *and Takeshi Endo*[a]

[1] Molecular Engineering Institute, Kinki University 11-6 Kayanomori, Iizuka, Fukuoka 820-8555 Japan.

[2] Kyushu Institute of Technology 2-4 Hibikino, Wakamatsu-ku, Kitakyushu-shi, Fukuoka, 808-0196, Japan.

*Corresponding author: Haruo Nishida

Tel / Fax: +81-948-22-5706.

E-mail address: hnishida@mol-eng.fuk.kindai.ac.jp (H. Nishida)

Abstract

To control the depolymerization of poly-L-lactic acid (PLLA) into L,L-lactide, effects of altering the physical and chemical properties of magnesium oxide (MgO) on its ability as a catalyst were investigated. Four kinds of MgO particles: MgO-heavy, 0.2, 0.05, and 0.01μm, were used having primary particles of different dimensions, surface areas, and chemical structures/species. Thermo-gravimetric profiles of PLLA/MgO composites shifted into a lower temperature range due to an increase in the catalytic surface area resulting from a decrease in the dimensions of the MgO particles. However, decreasing the dimensions caused frequent side reactions with unfavorable products: cyclic oligomers and meso-lactide, due to the presence of different chemical structures/species. Heat treatment of the MgO particles effectively suppressed the oligomer production and enhanced the L,L-lactide production, but also accelerated the meso-lactide production at lower temperatures. These results indicate that the surface properties of MgO considerably influence the depolymerization of PLLA, with the catalytic behavior of MgO controllable by heat treatment and selection of the depolymerization conditions.

Keywords:

poly(L-lactic acid); thermal degradation; depolymerization; magnesium oxide; catalyst; feedstock recycling

1. Introduction

Poly(L-lactic acid) [poly(L-lactide), PLLA], a well-known bioabsorbable and biodegradable material, is an attractive raw material produced from renewable resources such as corn [1], potato, and garbage [2]. Because of the advantage of having a carbon neutral, the use of PLLA in industrial fields has been rapidly increasing in the form of molded parts for personal computers [3-5], mobile phones [6], and automobiles [7,8]. It is also anticipated to have many other future applications where environmentally compatible materials are required, such as in mulching film and nursery boxes. However, PLLA needs a large amount of energy to be produced from the renewable resources and has poor biodegradability in certain environments [9]. Thus, other strategies for the effective use of PLLA are required.

PLLA is generally prepared by the ring-opening polymerization of L,L-lactide as a cyclic monomer [10-12], and during its thermal degradation L,L-lactide is recovered as a result of the depolymerization of PLLA (Scheme 1) [13,14]. This polymerization-depolymerization behavior is one of the special properties of PLLA and the depolymerization has actually been used as one method of producing L,L-lactide from oligomers in an industrial process [1]. Thus, this particular chemical property makes PLLA into a possible candidate for the feedstock recycling of plastics.

[**Scheme 1**]

However, the actual thermal degradation of PLLA is more complex than the simple reaction that gives L,L-lactide. For example, Duda et al. [14] and Witzke et al. [15] have reported the ceiling temperature and thermodynamic parameters for the equilibrium polymerization of lactide. In spite of these studies, the reported parameters were distributed over a wide range of values. The activation energy of degradation, E_a, has also been reported to change irregularly in a range of 70-270 kJ·mol^{-1} as the degradation progresses [16-18], and many kinds of degradation products have been detected during the pyrolysis of PLLA [16,19],

especially cyclic oligomers and their diastereoisomers.

Another serious difficulty with the feedstock recycling of PLLA is the racemization on lactate units, which generates optical isomers: *meso*- and D,D-lactides that cause serious problems on the reproduction of PLLA, diminishing its crystallizability (Scheme 1) and some other useful properties [16-18,20]. These examples illustrate that there are many mechanisms and factors that are influencing the depolymerization of PLLA. For feedstock recycling it is very important to control the mechanisms in the selective production of L,L-lactide from PLLA. If, through such control, the feedstock recycling to L,L-lactide as the monomer could be achieved, then PLLA would certainly become more widely used as a reasonable choice for a sustainable future society [21].

Recently, the effects of including a trace amount of metal as a polymerization catalyst, such as Sn, were investigated with the aim of clarifying the diversity of degradation behavior exhibited by PLLA [22-24]. In addition, some catalysts effective in controlling the depolymerization of PLLA have been developed [25,26]. MgO and $Al(OH)_3$ were the effective catalysts, under which PLLA was selectively depolymerized into L,L-lactide under specified conditions. In the case of $Al(OH)_3$, a large amount of the catalyst (30~50 wt%) is required for the depolymerization, because it mainly functions as a flame retardant [27]. On the other hand, only a small amount of MgO (<5 wt%) is required for the depolymerization [25], because it functions only as a depolymerization catalyst. Thus, MgO is expected to be a commonly usable catalyst for the feedstock recycling of PLLA.

In spite of the development of these effective catalysts, racemization remains as one of the serious problems associated with the feedstock recycling of PLLA, because, as has been recently found, the racemization of L,L-lactide is accelerated on the surface of basic catalysts [28]. Although the base strength of MgO is poor when compared to other alkaline earth oxides as shown by the following ranking: BaO>SrO>CaO>MgO [29], on the MgO surface the

presence of three different basic sites was indicated from profiles of CO_2-temperature programmed desorption [30]. The distribution of these basic sites depended on thermal treatment of MgO. Moreover, from FT-IR studies, four types of basic sites were proposed for MgO: (1) Mg-OH and three types of O^{2-} sites located on (2) edges, (3) vertices, and (4) pits on the surface [31].

To control the depolymerization of PLLA, modification of the catalytic function is required. In this paper, the effects on the PLLA depolymerization of the physical and chemical properties of MgO, such as particle dimension, surface area, and chemical structures on surfaces, were investigated through evaluation of the racemization.

2. Experimental

2.1 Materials

Polymer: PLLA (LACEA H-100J, Sn content: 40 ppm, M_n 98 000, M_w 170 000) was obtained from Mitsui Chemicals. Catalysts: four kinds of magnesium oxide particles (MgO-heavy, 0.2, 0.05, and 0.01μm), of differing particle dimensions, were purchased from Wako Pure Chemical Industries, Ltd. (Wako) (see Table 1). These catalysts were used after heat-treatment under prescribed conditions. Magnesium hydroxide ($Mg(OH)_2$) and basic magnesium carbonate ($MgCO_3 \cdot Mg(OH)_2 \cdot 4H_2O$) were purchased from Wako and used as received. Chloroform ($CHCl_3$) was obtained from Katayama Chemical and purified by extracting with 1**M** H_2SO_4 aq., washing by distilled water, refluxing over calcium chloride, and then distilling in a N_2 atmosphere.

2.2 Purification of PLLA

The as-received PLLA was purified in a three-stage process to remove the Sn ion; firstly dissolving the PLLA 15.0 g in chloroform 250 mL and extracting the residual Sn ion from the

PLLA/chloroform solution three times with 1 L of 1**M** HCl aqueous solution, then washing with distilled water until the aqueous phase became totally neutral, and finally precipitating the polymer with methanol to prepare the purified PLLA-H (Sn content: 7 ppm).

2.3 Heat treatment of MgO particles

MgO-heavy, 0.2, 0.05, and 0.01μm particles were heated in an AZ ONE programmable furnace MMF-1 at 120, 350, and 600 ºC for 2 h under air, and then cooled down gradually to room temperature in an air atmosphere. The heated MgO samples were stored in a desiccator until use.

2.4 Preparation of PLLA-MgO film samples

The five kinds of film samples (PLLA-H, PLLA-H/MgO-heavy, 0.2, 0.05, and 0.01μm) were prepared. A chloroform suspension (10 mL) of PLLA (400 mg) and MgO (20 mg) was stirred for 1.0 h at room temperature, and then cast in a glass Petri dish. After the evaporation of the solvent, the formed film was removed and then vacuum dried.

2.5 Characterization

Morphology of MgO particles was observed with a KEYENCE digital light microscope VH-5000 by a transmission method. Specific surface areas of MgO particles were measured by a standard BET method on a Mountech Co., Ltd. automatic surface area analyzer Macsorb HM model-1201 using a mixed gas: N_2/He = 30/70 (v/v) for the adsorption of N_2 molecules on the surfaces. Fourier transform infrared (FT-IR) spectroscopy was performed using a Nicolet Avatar 360 FT-IR spectrometer. Transmission spectra of the heat-treated MgO samples were measured by a KBr disk method.

2.6 Thermal degradation of blend and composite samples

Thermal degradation behavior of PLLA was analyzed by the thermogravimeter (TG) and the pyrolysis-gas chromatograph/mass spectrometer (Py-GC/MS). TG was conducted on a Seiko Instrumental Inc. EXSTAR 6200 TG/DTA system in an aluminum pan (5 mm Æ) under a constant nitrogen flow (100 mL·min^{-1}) using about 3-5 mg of film sample. Dynamic thermal degradation of the sample was conducted at prescribed heating rates, Æ, of 1, 3, 5, 7, and 9 °C·min^{-1} in a temperature range of 60 to 500 °C. The thermal degradation data were collected at regular intervals (about 20 times per degree) by an EXSTAR 6000 data platform and recorded into an analytical computer system.

Py-GC/MS was conducted on a Frontier Lab PY-2020D double–shot pyrolyzer connected to a Shimadzu GC/MS-QP5050 chromatograph/mass spectrometer, which was equipped with an Ultra Alloy^{+}-5 capillary column (30 m × 0.25 mm i.d.; film thickness, 0.25 μm). High purity helium was used as a carrier gas under a constant flow of 100 mL·min^{-1}. In the dynamic heating process with Py-GC/MS, about 0.5 mg of sample was added to the pyrolyzer and heated from 60°C to a prescribed temperature at a heating rate of 9 °C·min^{-1}. Volatile pyrolysis products were introduced into the GC through a selective sampler. The temperature of the column oven was first set at 40 °C. After the pyrolysis process had finished, the column was heated according to the following program: 40 °C for 1 min, 40-120 °C at 5 °C·min^{-1}, 120-320 °C at 20 °C·min^{-1}, and 320 °C for 13 min. Mass spectrum measurements were recorded 2 times·s^{-1} during this period.

3. Results and Discussion

3.1 Morphology of MgO particles

Magnesium oxide (MgO) exhibits a simple rock salt structure and may easily be produced as a high surface area material [32]. Four kinds of MgO particles, i.e., MgO-heavy, 0.2, 0.05, and

0.01μm, were used for this study as catalysts of PLLA depolymerization. The differences between MgO-heavy and MgO-0.2 ~ 0.01μm result from a difference in calcination temperature in their production processes. Morphology of the MgO particles was observed with a digital light microscope. Results are listed in Table 1. As expected, the smaller the dimension of the primary particle, the larger its surface area. In a depolymerization process of PLLA, the area of MgO particle surface acting as the catalytic area must be related to the rate of depolymerization. Secondary particles of MgO-heavy had a columnar crystal structure. On the other hand, other secondary particles of MgO were aggregates of powdery primary particles, having diverse shapes. The smaller the dimensions of the primary particle became, the larger became the dimensions of the secondary particle. This indicates that the smaller particles easily aggregate to form larger secondary particles. This easy aggregation property of the smaller particles was also observed in composites with PLLA. In a PLLA matrix, the smaller particles formed large amorphous-like aggregates.

Each of the MgO particles was mixed with PLLA-H in a solution of $CHCl_3$ under vigorous stirring, and then the mixed solution was cast on a glass surface, resulting in a homogeneous sample film. Dispersibility of the MgO particles in the PLLA matrix was determined by microscopic observation of the obtained films (Figure 1), which were melted and stretched prior to observation. As shown in Figure 1, it was found that MgO-heavy and 0.2μm particles dispersed without additional aggregation of the original secondary particles, but MgO-0.05 and 0.01μm particles aggregated to give a larger size distribution than that of the original secondary particles.

[**Table 1**]

[**Figure 1**]

3.2 Thermal degradation behavior of PLLA in the presence of various MgO particles

To compare the catalytic activity of the four kinds of MgO particles having different dimensions, the thermal degradation of PLLA was carried out with TG and Py-GC/MS using

PLLA-H/MgO (120°C) composite films: PLLA-H:MgO=100/5 (wt/wt), in which the MgO (120°C) particles were heat-treated at 120 °C for 2 h beforehand. TG profiles are illustrated in Figure 2. The TG profile shifted into a lower temperature range; the maximum shifting by 35 °C, with a decrease in the dimension of the MgO particle. This result must be due to the increase in the catalytic surface area of MgO particles. Generally, a shift in the degradation range into a temperature range below 300 °C suggests the effective suppression of racemization, because the racemization on the polymer chain easily occurs at temperatures over 300 °C to produce diastereoisomers, such as meso and D,D-lactides.

[**Figure 2**]

Pyrolysis products from the PLLA-H/MgO (120°C) samples were analyzed with Py-GC/MS in temperature ranges of 60 °C to prescribed temperatures by increasing the maximum temperature stepwise by 10 °C to 310 °C. Results are shown in Figure 3. All the samples gave L,L-lactide, meso-lactide, and cyclic oligomers as pyrolysis products. The amounts of meso-lactide and cyclic oligomers increased with increase in the temperature. Interestingly, PLLA-H/MgO-0.2, 0.05, and 0.01μm film samples afforded more unfavorable products than those from PLLA-H/MgO-heavy, in spite of the degradation in lower temperature ranges as shown in Figure 2. In particular, PLLA-H/MgO-0.01μm gave a large amount of meso-lactide even at 260~270 °C. These results indicate that as the dimensions of the MgO particle are reduced there is an increase in the number of side reactions giving unfavourable products at lower temperatures.

The cyclic oligomers are produced as a result of the intra-molecular trans-esterification reactions between an active chain end and an ester group in the same chain. On the other hand, meso-lactide production results from an ester-semiacetal tautomerization on a polymer chain [16] and a following ring-forming reaction, or a back-biting reaction from an active chain end: $R\text{-}COO^-$ [33]. The generated cyclic oligomers, including lactides, vaporize at appropriate

temperatures through a process of fractional distillation. Thus, the results in Figure 3 may result from the fractional distillation of a range of generated cyclic oligomers.

[**Figure 3**]

3.3 Characterization of surfaces of MgO particles

The acceleration of various side reactions by the MgO particles with small dimensions suggests the presence of some kinds of active sites on the MgO surfaces. To analyze the chemical structures/species on the surfaces of the MgO particles, FT-IR analysis was employed using a KBr disk method. FT-IR transmission spectra of MgO-0.2, 0.05, and 0.01μm (120°C) are illustrated in Figure 4. The spectra of the MgO (120°C) particles were normalized based on the absorbance of Mg-O bond vibration in a range of 450-700 cm^{-1} [34,35]. Other absorption bands, centered around 3400-3500 cm^{-1} for ½OH and 1470 cm^{-1} for ½OCO, were also particularly evident on the spectrum of MgO-0.01μm. These absorptions originated from different chemical structures/species, such as Mg-OH, adsorbed H_2O, Mg-CO_3H, and Mg-O-CO-O-Mg on the surface of MgO particles [32].

These different structures/species, especially Mg-OH and adsorbed H_2O, must cause the random degradation of PLLA, which then produces a large amount of oligomers and active chain end structures: -COO^- $^+$Mg, -COOH, and –OH. These active chain ends attack the intra-molecular ester bonds, resulting in the production of diastereoisomers of cyclic oligomers including L,L- and meso-lactides [33].

[**Figure 4**]

3.4 Changes in chemical structures on MgO particle surfaces during heating

To estimate effects of the chemical structures/species on the MgO particle surface, thermal degradation behavior of intact MgO particles, $Mg(OH)_2$ and basic $MgCO_3$:

{$MgCO_3 \cdot Mg(OH)_2 \cdot 4H_2O$} as control materials was examined by TG (Figure 5). MgO particles showed decreases in weight in two steps in temperature ranges of r.t.-150 °C and 200-320 °C. In particular, the weight loss of MgO-0.01μm during the heating process was remarkable. $Mg(OH)_2$ showed a one-step weight-loss to change into MgO in a temperature range of 260-350 °C. Basic $MgCO_3$ exhibited a two weight loss process in the temperature ranges 200-300 °C and 350-450 °C, *i.e.* the first step was the dehydration/decarboxylation step from basic $MgCO_3$ to $MgCO_3$ and MgO, and the second step was the CO_2 elimination from $MgCO_3$ to give MgO. Taking account of the weight-loss behavior of $Mg(OH)_2$ and basic $MgCO_3$, the observed two-step weight-loss process of the MgO particles must involve the evaporation of adsorbed H_2O as a first step and the dehydration/decarboxylation from $MgCO_3H$ Mg-OH groups as a second step. The total weight loss values of the MgO particles up to 600 °C are listed in Table 1. These values indicate clearly that the smaller MgO particles have a greater number of different chemical structures/species on their surfaces.

[**Figure 5**]

The weight loss of MgO particles under heating must be accompanied by some changes not only in their chemical structure, but also in their catalytic behavior during the thermal degradation of PLLA. The changes in the chemical structures of MgO particles were examined with FT-IR after heat treatments at 350 and 600 °C for 2 h under air in a programmable furnace. Typical changes in FT-IR spectra of MgO-0.2 and 0.01μm are shown in Figure 6. In this figure, the absorbance of the spectra is given as a relative value, which has been normalized so as to be equal to the maximum absorbance of Mg-O bond vibration in a range of 460-700 cm^{-1}. As shown in Figure 6, the broad absorption at 1300-1600 cm^{-1} for ν_{CO} of –Mg-CO_3H and –Mg-CO_3-Mg- markedly decreased with temperature in both samples. On the other hand, for the changes in the absorption centered around 3400-3500 cm^{-1} for ν_{OH} of Mg-OH and adsorbed H_2O a difference in behavior was evident between the MgO-0.2 and

0.01μm particles. Although the absorption for ν_{OH} of MgO-0.2μm particles steadily decreased with the temperature (Figure 6(a)), the absorption of MgO-0.01μm particles was not steady and actually increased a little after heat-treatment at 600 °C (Figure 6(b)). MgO-heavy particles showed the same behavior to that of MgO-0.2μm, whilst MgO-0.05μm particles exhibited a behavior midway between that of MgO-0.2 and 0.01μm particles. These results suggest either that it is difficult to change small MgO particles with large surface area into a typical Mg-O-Mg structure from surface Mg-OH groups under the heating conditions, or that it is easy to recover the Mg-OH and/or Mg-CO_3H structures from temporarily formed Mg-O-Mg structures during the cooling process in the presence of air.

[**Figure 6**]

3.5 Thermal degradation behavior of PLLA in the presence of heat-treated MgO particles

To determine the changes in catalytic activity of heat-treated MgO (HT-MgO) particles, the thermal degradation behavior of PLLA was investigated using PLLA-H/HT-MgO (350°C) and (600°C) (100/5 (wt/wt)) composite films by using TG and Py-GC/MS. Results were compared with those of PLLA-H/MgO (120°C) (100/5 (wt/wt)) composite films. The TG profiles are illustrated in Figure 7. TG profiles of PLLA-H/HT-MgO composites did not change very much after the heat treatments. These results suggest that the total number of active sites for the PLLA degradation on the MgO particle surfaces does not significantly change before and after the heat treatments.

[**Figure 7**]

Pyrolysis products from PLLA-H/HT-MgO (350°C) and (600°C) composite films were analyzed with Py-GC/MS under the same conditions as the pyrolysis products from PLLA-H/MgO (120°C) composite films. Results are illustrated in Figure 8. Although the cyclic oligomers were generated from all the PLLA-H/MgO (120°C) samples, the heat

treatments of MgO particles at 350 and 600 °C effectively suppressed the production of the cyclic oligomers so as to make them hardly visible, resulting in enhanced L,L-lactide production on the pyrolysis of the film samples. Interestingly, in the cases of PLLA-H/HT-MgO-0.05 and 0.01μm composite films the temperature at which meso-lactide began to be produced shifted to lower temperatures with increase in the temperature of heat treatment. However, no temperature shift for the meso-lactide production was observed in the case of PLLA-H/HT-MgO-0.2μm.

The above results suggest that new active sites for meso-lactide production were formed during the heat-treatments, while the active sites for oligomer production mostly disappeared or were made inactivate. Possible reaction mechanisms for the depolymerization of PLLA-H/MgO composite films are illustrated in Scheme 2. The oligomer production may be caused by Mg-OH groups, adsorbed H_2O, and generated H_2O from the dehydration of Mg-OH groups. These H_2O molecules can produce a large amount of linear oligomers by random degradation, and in a following intra-molecular transesterification at higher temperatures cyclic oligomers must be produced. On the other hand, the Mg-OH group react with an ester group to give a salt structure, $–COO^-\ ^+Mg$, and a new alcohol end structure. During this reaction, racemization may occur at the alcoholic end group. These end structures: $–COO^-\ ^+Mg$ and the racemized alcoholic group will produce diastereoisomers including meso-lactide by intra-molecular transesterification. Therefore, it is considered that the lower-temperature shift of meso-lactide production as shown in Figure 8 is caused by Mg-OH groups. Moreover, it is assumed that the carbonate structures: MgO-CO-OMg and $MgCO_3H$, protect the Mg-OH to inhibit the unfavorable meso-lactide production. At higher temperatures, to be able to eliminate the carbonate groups such as at 600°C, the protection of carbonate groups was removed and resulted in the acceleration of meso-lactide formation.

Based on this consideration, to maintain control into high-selective L,L-lactide

production from PLLA, more precise modification of the MgO particle surface will be required. The investigation of the effects of carbonate structures on MgO particle surfaces is now in progress. A report on this will follow in the near future.

[**Figure 8**]

[**Scheme 2**]

4. Conclusions

Four kinds of MgO particles, MgO-heavy, 0.2, 0.05, and 0.01μm were used for the thermal degradation of PLLA as depolymerization catalysts. The TG profile of PLLA shifted into a lower temperature range; the maximum shifting by 35 °C, with the decrease in the dimensions of MgO particles, reflecting the increase in catalytic surface area. However, as the dimensions of MgO particles were reduced, side reactions occurred more frequently to give the unfavorable products, cyclic oligomers and meso-lactide. The FT-IR analysis of MgO particles clarified the presence of some different chemical structures/species, such as Mg-OH, adsorbed H_2O, and $MgCO_3$ species, which may cause the unfavorable side reactions. The heat treatments of MgO particles at temperatures of 350 and 600 °C effectively suppressed the oligomer production and so enhanced the L,L-lactide production. However, especially in the case of MgO-0.01μm, the heat treatments accelerated the meso-lactide production at low temperatures. These results indicate that the catalytic behavior of MgO particles on PLLA depolymerization is considerably influenced by the surface area and different chemical structures/species on the MgO particle surfaces. To achieve control into high-selective L,L-lactide production from PLLA, more precise modification of MgO particle surface will be required.

References

[1] Lunt J. Large-scale production, properties and commercial applications of polylactic acid polymers. Polym Degrad Stab 1998;59:145-152.

[2] Shirai Y, Sakai K, Miura S, Ohara H. Production of poly-lactate from kitchen refuse in Japan. Proceedings International Symposium on Biotechnology for Recycling of Organic Wastes to Useful Resources 2001;7-9.

[3] NEC succeeds in development of flame resistant bio-plastic. Mod Plast Int 2004;34:60.

[4] Serizawa S, Inoue K, Iji M. Kenaf-fiber-reinforced poly(lactic acid) used for electronic products. J Appl Polym Sci 2006;100:618-624.

[5] Kimura K. Large-sized plastic case constituting of biomaterials for note-type computer. Japan Plastics 2005;56:72-76.

[6] Iji M. Application of advanced bio-plastic to electric appliances. Expected Materials for the Future 2006;6:22-26.

[7] Isobe Y, Ino T, Kageyama Y, Nakano M, Usuki A. Improvement of heat resistance for bioplastics. Special Publications Soc Automotive Eng 2003;SP-1763:103.

[8] Riedel U, Nickel J. Natural fibre-reinforced biopolymers as construction materials – new discoveries. Angew Makromol Chem 1999;272:34-40.

[9] Tokiwa Y, Jarerat A. Microbial degradation of aliphatic polyesters. Macromol Symp 2003;201:283-289.

[10] Leenslag JW, Pennings AJ. Synthesis of high-molecular-weight poly(L-lactide) initiated with tin 2-ethylhexanoate. Macromol Chem 1987;188:1809-1814.

[11] Kricheldorf HR, Kreiser-Saunders I, Stricker A. Polylactones 48. SnOct2-initiated polymerization of lactide: a mechanistic study. Macromolecules 2000;33:702-709.

[12] Kowalski A, Duda A, Penczek S. Polymerization of L,L-lactide initiated aluminum

isopropoxide trimer or tetramer. Macromolecules 1998;31:2114-2122.

[13] Nomura N, Ishii R, Akakura M, Aoi K. Stereoselective ring-opening polymerization of racemic lactide using aluminum-achiral ligand complexes: Exploration of a chain-end control mechanism. J Am Chem Soc 2002;124:5938-5939.

[14] Duda A, Penczek S. Thermodynamics of L-lactide polymerization. Equilibrium monomer concentration. Macromolecules 1991;23:1636-1639.

[15] Witzke DR, Narayan R, Kolstad JJ. Reversible kinetics and thermodynamics of the homopolymerization of L-lactide with 2-ethylhexanoic acid tin(II) salt. Macromolecules 1997;30:7075-7085.

[16] Kopinke FD, Remmler M, Mackenzie K, Moder M, Wachsen O. Thermal decomposition of biodegradable polyesters-II. Poly (lactic acid). Polym Degrad Stab 1996;53:329-342.

[17] Babanalbandi A, Hill DJT, Hunter DS, Kettle L. Thermal stability of poly(lactic acid) before and after ^{3}-radiolysis. Polym Int 1999;48:980-984.

[18] Aoyagi Y, Yamashita K, Doi Y. Thermal degradation of poly[(R)-3-hydroxybutyrate], poly [μ-caprolactone], and poly[(S)-lactide]. Polym Degrad Stab 2002;76:53-59.

[19] McNeill IC, Leiper HA. Degradation studies of some polyesters and polycarbonates-2. Polylactide: Degradation under isothermal conditions, thermal degradation mechanism and photolysis of the polymer. Polym Degrad Stab 1985;11:309-326.

[20] Ajioka M, Enomoto K, Suzuki K, Yamaguchi A. Basic properties of polylactic acid produced by the direct condensation polymerization of lactic acid. Bull Chem Soc Jpn 1995;68:2125-2131.

[21] Fan Y, Nishida H, Shirai Y, Endo T. Control of racemization for feedstock recycling of PLLA. Green Chemistry 2003;5:575-579.

[22] Nishida H, Mori T, Hoshihara S, Fan Y, Shirai Y, Endo T. Effects of tin on poly(L-lactic

acid) pyrolysis. Polym Degrad Stab 2003;81:515-523.

[23] Fan Y, Nishida H, Shirai Y, Endo T. Thermal Stability of Poly (L-lactide): Influence of End Protection by Acetyl Group. Polym Degrad Stab 2004;84:143-149.

[24] Abe H, Takahashi N, Kim KJ, Mochizuki M, Doi Y. Thermal degradation processes of end-capped poly(L-lactide)s in the presence and absence of residual zinc catalyst. Biomacromolecules 2004;5:1606-1614.

[25] Fan Y, Nishida H, Mori T, Shirai Y, Endo T. Thermal degradation of poly (L-lactide): Effect of alkali earth metal oxides for selective L,L-lactide formation. Polymer 2004;45:1197-1205.

[26] Nishida H, Fan Y, Mori T, Oyagi N, Shirai Y, Endo T. Feedstock recycling of flame-resisting poly(lactic acid) / aluminum hydroxide composite to L,L-lactide. Ind Eng Chem Res 2005;44:1433-1437.

[27] Sterzel, H.-J. Flammwidrig ausgerüstetes polylactid und copolylactid. DE Patent 4,325,849 A1, 1993.

[28] Tsukegi T, Motoyama T, Shirai Y, Nishida H, Endo T. Racemization Behavior of L,L-Lactide during Heating. Polym Degrad Stab, submitted.

[29] Zhang Z, Hattori H, Tanabe K. Aldol addition of acetone, catalyzed by solid base catalysts; magnesium oxide, calcium oxide, strontium oxide, barium oxide, lanthanum(III) oxide and zirconium oxide. Appl Catal 1989;36:189-197.

[30] Wang GW, Hattori H. Reaction of adsorbed carbon monoxide with hydrogen on magnesium oxide. J Chem Soc Faraday Trans I 1984;80:1039-1047.

[31] Hattori H. Catalysis by basic metal oxides. Materials Chem Phys 1988;18:533-552.

[32] Knözinger E, Jacob KH, Singh S, Hofmann P. Hydroxyl groups as IR active surface probes on MgO crystallites. Surf Sci 1993;290:388-402.

[33] Fan Y, Nishida H, Shirai Y, Endo T. Racemization on Thermal Degradation of

Poly(L-lactide) with Calcium Salt End Structure. Polym Degrad Stab 2003;80:503-511.

[34] Mekhemer GAH, Halawy SA, Mohamed MA, Zaki MI. Ketonization of acetic acid vapour over polycrystalline magnesia: in situ Fourier transform infrared spectroscopy and kinetic studies. J Catal 2005;230:109-122.

[35] Mironyuk IF, Gun'ko VM, Povazhnyak MO, Zarko VI, Chelyadin VM, Leboda R, Skubiszewska-Zi•va J, Janusz W. Magnesia foumed on calcination of Mg(OH)2 prepared from natural bischofite. Appl Surf Sci 2006;252:4071-4082.

Scheme and Figure Captions

Scheme 1. Polymerization-depolymerization behavior of PLLA.

Scheme 2. Possible thermal degradation pathways of PLLA/MgO particle composite films.

Figure 1. Microscopic images of MgO particles in PLLA-H/MgO composites.

Figure 2. TG profiles of various PLLA-H/MgO (120°C) (100/5 wt/wt) film samples. Samples: PLLA-H, PLLA-H/MgO-heavy, 0.2μm, 0.05μm, and 0.01μm. Heat treatment of MgO: at 120 °C for 2h. TG measurement: Æ= 9 °C·min^{-1}.

Figure 3. Py-GC/MS analysis of pyrolysis products from PLLA-H and PLLA-H/MgO (120°C) film samples.

Figure 4. FT-IR spectra of MgO (120°C) particles: MgO-0.2μm (solid line), MgO-0.05μm (broken line), and MgO-0.01μm (dotted line).

Figure 5. TG profiles of as-received MgO particles, $Mg(OH)_2$ and basic $MgCO_3$. Æ = 9 °C·min^{-1}.

Figure 6. FT-IR spectra of heat-treated MgO particles. (a) MgO-0.2μm and (b) MgO-0.01μm. Heat treatments at 120°C (dotted lines), 350°C (broken lines), and 600°C (solid lines).

Figure 7. TG profiles of PLLA-H/HT-MgO-0.2, 0.05, and 0.01μm (100/5 wt/wt) film samples. Heating conditions of MgO particles: at 120 (dotted lines), 350 (broken lines), and 600 °C (solid lines) for 2 h. TG measurement: *Æ*= 9 °C·min^{-1}.

Figure 8. Py-GC/MS analysis of pyrolysis products from PLLA-H/HT-MgO (350°C) and (600°C)-0.2, 0.05, and 0.01μm film samples.

Schemes and Figures

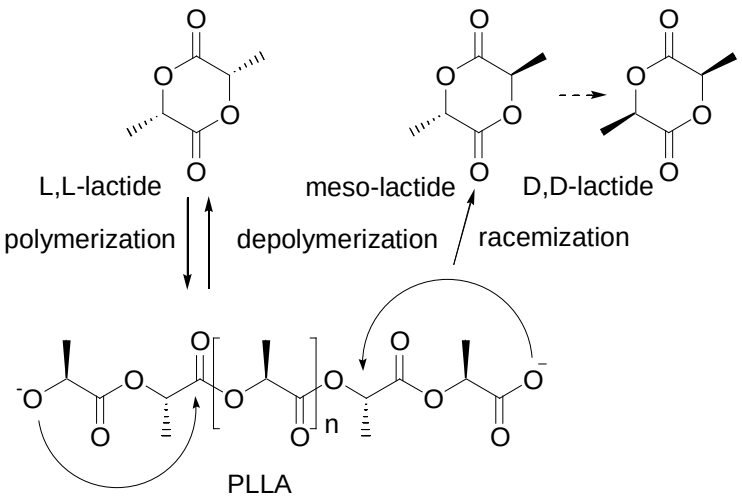

Scheme 1. Polymerization-depolymerization behavior of PLLA.

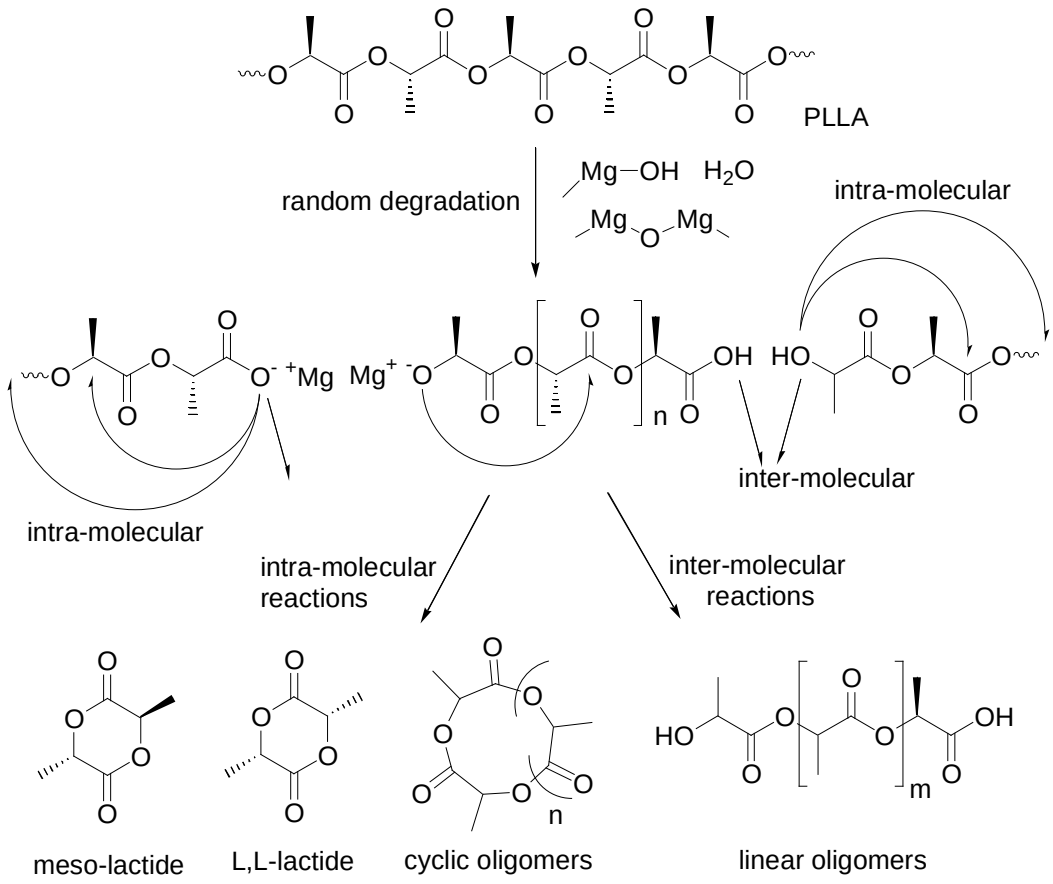

Scheme 2. Possible thermal degradation pathways of PLLA/MgO particle composite films.

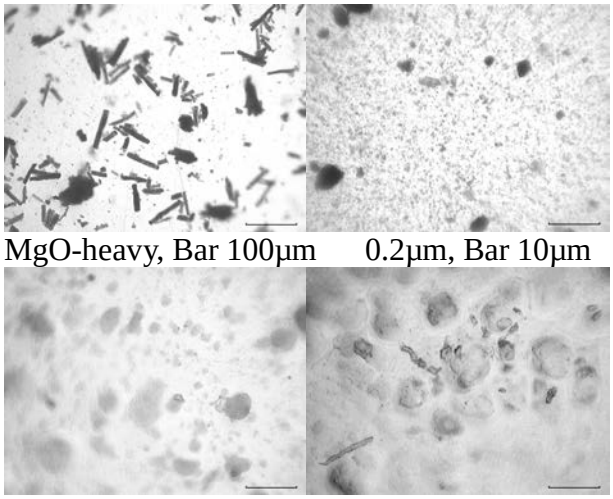

Figure 1. Microscopic images of MgO particles in PLLA-H/MgO composites.

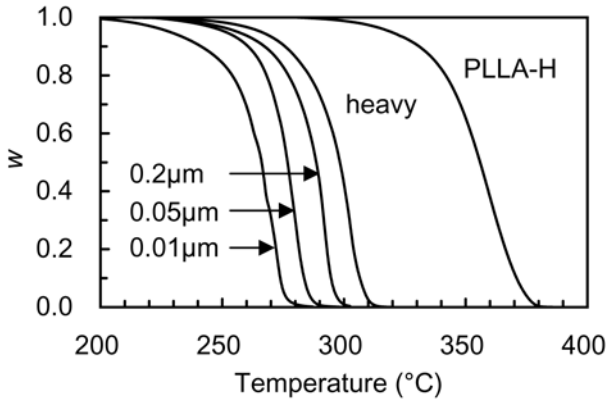

Figure 2. TG profiles of various PLLA-H/MgO (120°C) (100/5 wt/wt) film samples. Samples: PLLA-H, PLLA-H/MgO-heavy, 0.2μm, 0.05μm, and 0.01μm. Heat treatment of MgO: at 120 °C for 2h. TG measurement: Æ= 9 °C·min^{-1}.

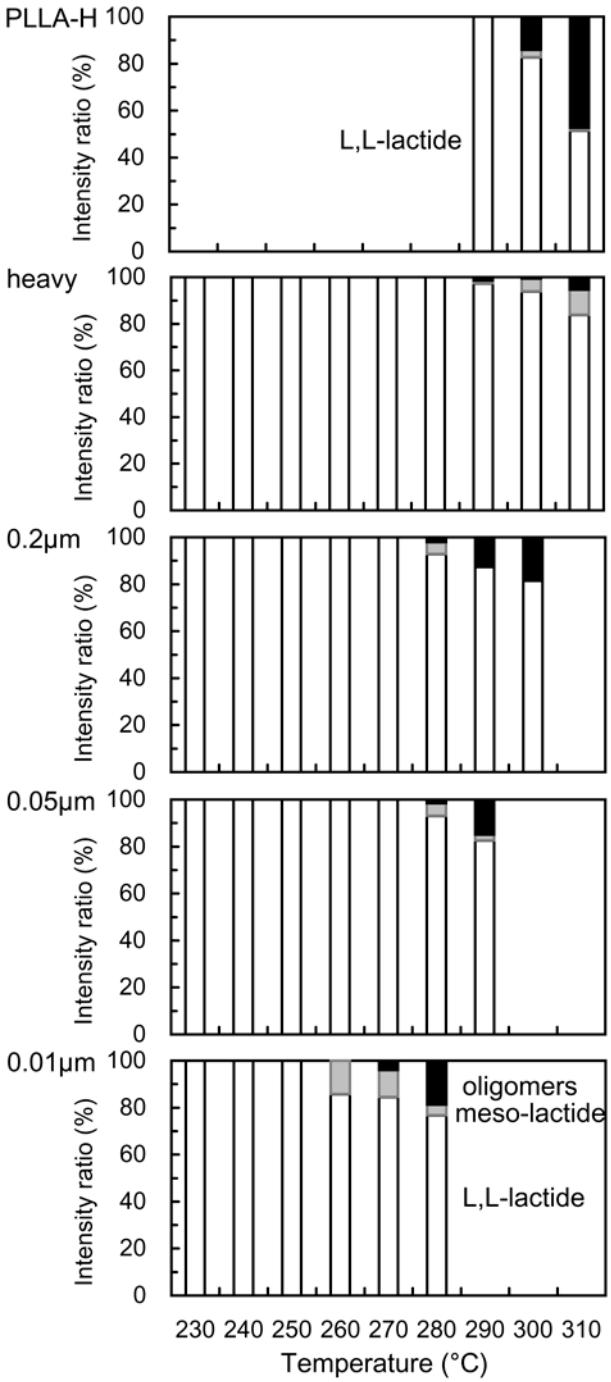

Figure 3. Py-GC/MS analysis of pyrolysis products from PLLA-H and PLLA-H/MgO (120°C) film samples.

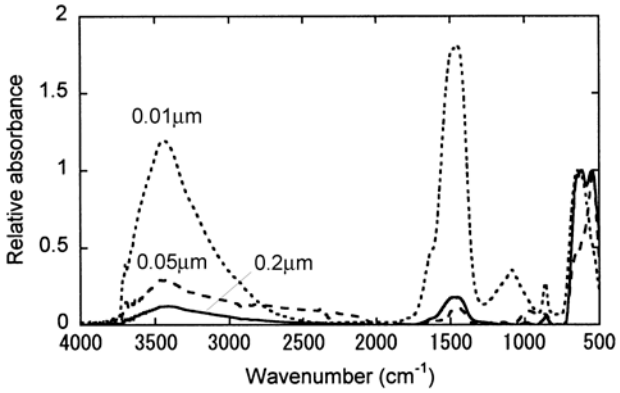

Figure 4. FT-IR spectra of MgO (120°C) particles: MgO-0.2μm (solid line), MgO-0.05μm (broken line), and MgO-0.01μm (dotted line).

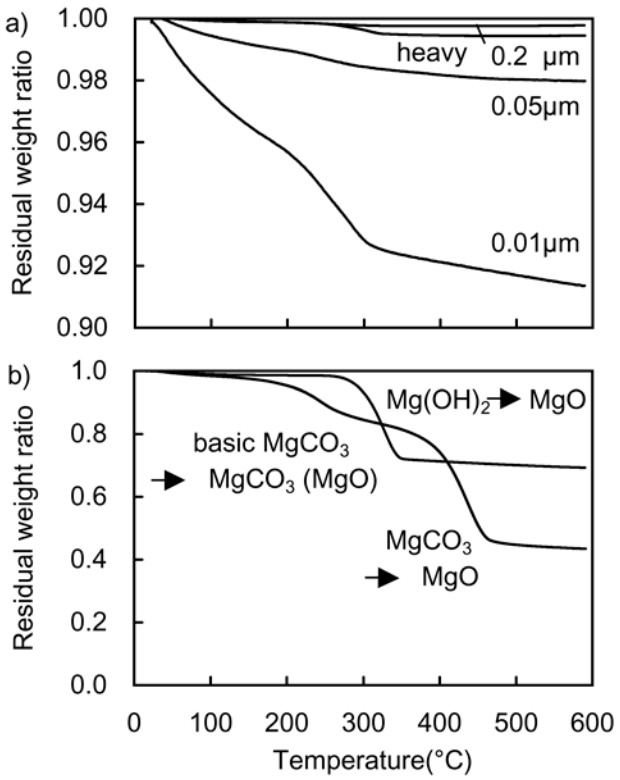

Figure 5. TG profiles of as-received MgO particles, $Mg(OH)_2$, and basic $MgCO_3$. *Æ* = 9 °C·min^{-1}.

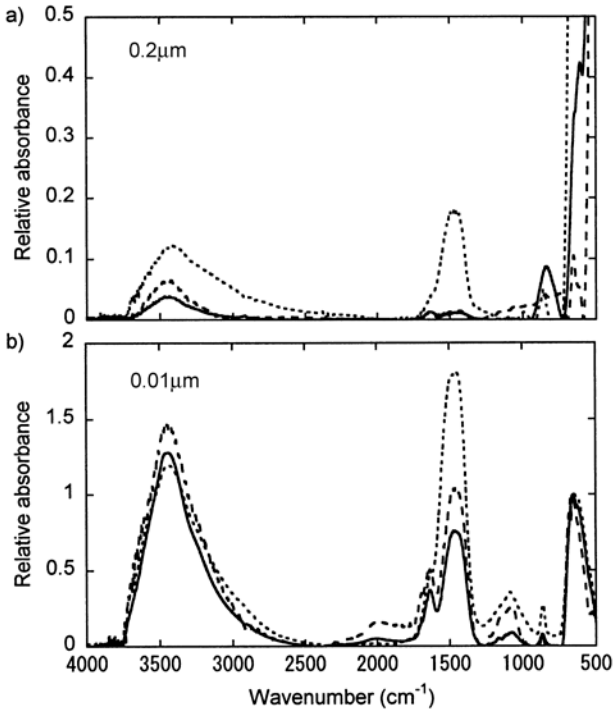

Figure 6. FT-IR spectra of heat-treated MgO particles. (a) MgO-0.2µm and (b) MgO-0.01µm. Heat treatments at 120°C (dotted lines), 350°C (broken lines), and 600°C (solid lines).

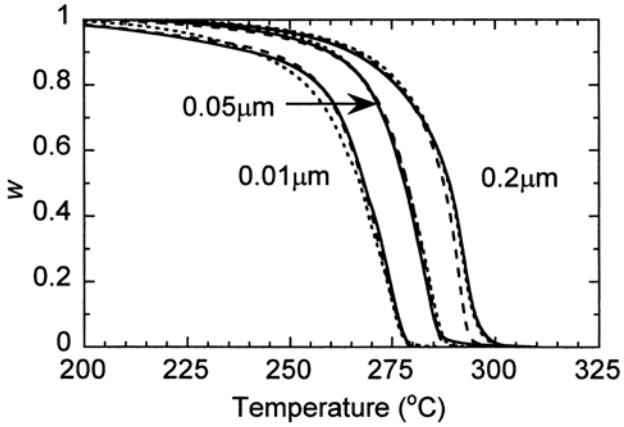

Figure 7. TG profiles of PLLA-H/HT-MgO-0.2, 0.05, and 0.01μm (100/5 wt/wt) film samples. Heating conditions of MgO particles: at 120 (dotted lines), 350 (broken lines), and 600 °C (solid lines) for 2 h. TG measurement: *Æ*= 9 °C·min^{-1}.

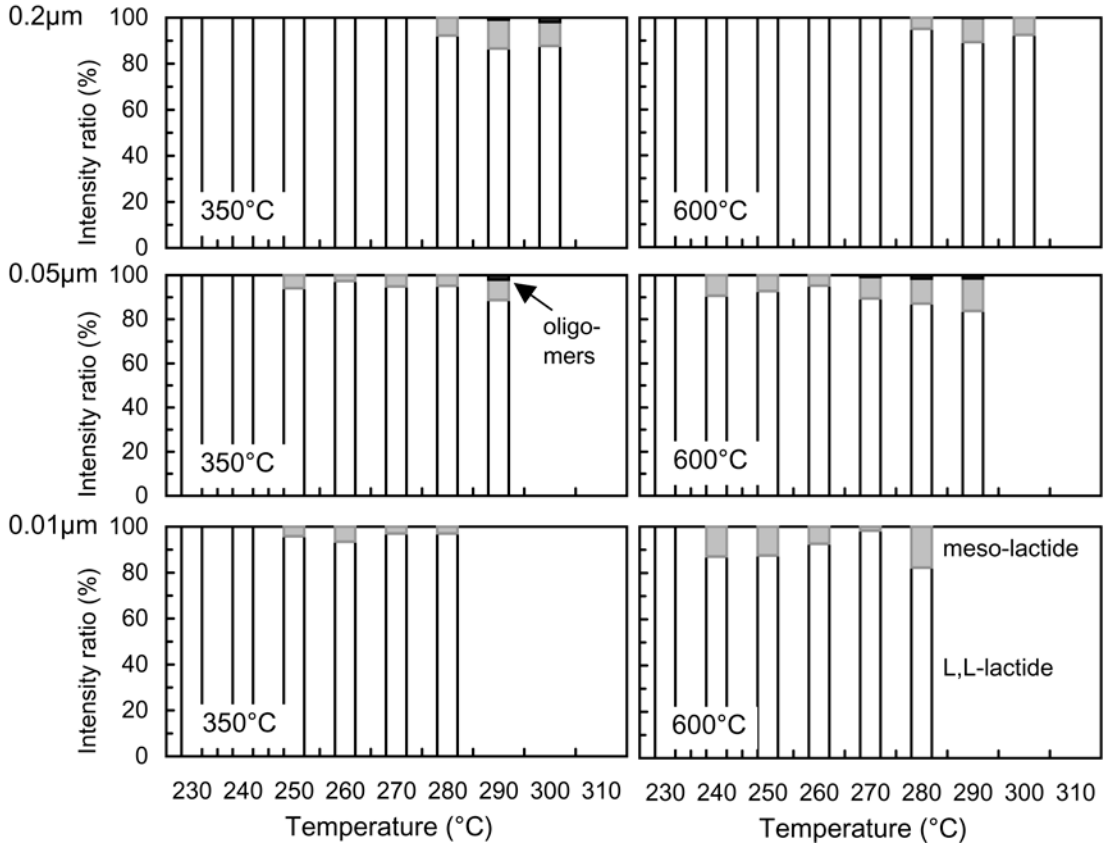

Figure 8. Py-GC/MS analysis of pyrolysis products from PLLA-H/HT-MgO (350°C) and (600°C)-0.2, 0.05, and 0.01μm film samples.

Tables

Table 1. Physical properties of MgO particles as depolymerization catalysts

MgO	morphology average dimension of particle (μm)		surface area [a] ($m^2 \cdot g^{-1}$)	weight loss during heating process [b] (wt%)
	primary particle	secondary particle		
heavy	regular hexahedron ¦ [c] = 0.5	columnar crystal 10 × 10 × 70	3	0.55
0.2μm	regular hexahedron ¦ = 0.2	aggregate ¦ = 1.2	7	0.22
0.05μm	regular hexahedron ¦ = 0.05	aggregate ¦ = 6.3	32	2.02
0.01μm	undetectable	aggregate ¦ = 10.9	181	8.64
$Mg(OH)_2$	-	-	-	30.73
basic $MgCO_3$	-	-	-	56.56

[a] Measured by a standard BET method using a mixed gas: N_2/He = 30/70 (v/v).
[b] Heating with TG from 60 to 600 °C at 9 °C·min^{-1}. [c] Average diameter.